XLIII CILAMCE
21–25, November, 2022
FOZ DO IGUAÇU – PR – BRAZIL

Passive control of plate vibrations: dimensional optimization of constrained layers by using kriging surrogate

Sandmara Lanhi[1], Gabriela W.O. Dicati[1], José E. Gubaua[1], Jucélio T. Pereira[2]

[1] *Laboratory of Computational Solid Mechanics*
Postgraduate Program in Mechanical Engineering (PG-Mec)
Federal University of Paraná, Polytechnic Center, 100 Cel. Francisco H. dos Santos, Curitiba PR 81530-000
sandmara_lanhi@hotmail.com; gabioening@gmail.com; gubaua@ufpr.br
[2] *Laboratory of Computational Solid Mechanics*
Postgraduate Program in Mechanical Engineering (PG-Mec)
Federal University of Paraná, Polytechnic Center, 100 Cel. Francisco H. dos Santos, Curitiba PR 81530-000
Dept. Mechanical Engineering, Federal University of Paraná, Curitiba, Brazil
jucelio.tomas@ufpr.br

Abstract. Plate structures are slender and flexible structures and can be subject to vibrations. Vibrations can cause problems such as acoustic discomfort, mechanical fatigue failure, and/or reduced performance. Thus, it is necessary to use forms of control that aim to reduce and avoid vibration. One method is the passive vibration control using constrained layers (CL). This method stands out due to easily and simplicity of application. In this control form, the vibrating structure receives a layer of viscoelastic material (VEM) and a material layer, usually metallic. For efficient vibration control, it is necessary to determine the optimal parameters of the CL. Thus, this work aims to present a methodology for optimizing the vibration control of a plate using CL and Kriging's surrogate. Considering the width and length of the VEM fixed, the design variables of this problem are the thickness of the constrained layer (VEM) and constraining layer (metallic layer). The CL kept dimension and shape fixed during the optimization process. The objective function evaluated is the Euclidean norm of a component of the matrix function of inertance. As a result, we obtained optimal thicknesses of VEM and restrictor layers for effective control of the second and third vibration modes.

Keywords: passive vibration control, viscoelastic material, Kriging metamodel.

1 Introduction

Plate structures are plane and slender elements. These elements are present in cars, airplanes, shifts, machines, and pieces of equipment. The plate structures are flexible and support statical and dynamic loads, mainly perpendicular to the middle surface, which generates bending. Also, they are susceptible to vibrations [1]. The vibrations can cause acoustic discomfort, failure by fatigue, and reduction of performance. Thus, it is necessary to apply methods to decrease or avoid vibrations in plate structures. One method is passive vibration control using constrained layers (CL). This method stands out due to easily and simplicity of application. The CL provides meaningful damping effects in wide frequency and temperature ranges.

The passive control by CL consists of adding a composite structure with a viscoelastic material (VEM) sandwiched between the vibrant structure (or base structure) and a metallic constraining layer. Thus, when the base structure vibrates, the VEM layer dissipates the vibration energy through heat. This dissipation occurs due to the shear deformation of VEM, caused by the difference in displacements between the constraining layer and base structure [1,2]. The CL has been an effective tool for controlling the vibrations in [3-5]. Bending movement is the result when plate structures vibrate. This type of movement favors the shear deformation of the constrained layer.

Usually, a percentage of the CL's area covers the base structure. It is impossible to cover the entire vibrant surface. This type of covering can compromise its performance. Another factor is the thicknesses of the VEM and constraining layers. They act in the capability of damping and noise control of CL. The large size of the thicknesses influences the cost and the weight of the CL [3-5].

This study aims to present an optimization methodology for passive control using CL. For this, we use an optimization technique based on the Kriging surrogate. The objective function considers the Euclidean norm of a component of the matrix function of inertance. The design variables of the optimization process are the thicknesses of the VEM and the constraining layers. We performed two cases for a fixed-right-edge base structure. We considered a maximum size of 30% of the area of the base structure to determine the covered area by the CL. Initially, we used a CL centralized on the base structure. Also, we modeled the CL longitudinally disposed on the base structure. However, the CL extended and centralized itself along the length and width of the base structure. For both CLs, the frequency ranged from 0 to 580 Hz.

2 Methodology

The methodology of this work uses the concept of metamodeling by Kriging to determine the thicknesses of the VEM and constraining layer used to perform the plate passive control.

2.1 Optimization process

The structure for optimization of the thicknesses of the VEM and the constraining layer follows the flowchart presented in Fig 1. The computational model uses the Abaqus and Matlab software packages to execute the optimization process. The Matlab software runs the optimization process based on a surrogate. The Abaqus software performs numerical simulations through the Finite Element Method (FEM) to obtain the numerical data that quantifies the objective function.

We used the Simple Kriging [6,7] as surrogate in the methodology proposed. In this sense, a given random process, $Y(x)$, is defined by the sum between the known trend function, $\mu(x)$, and a centered random process, $Z(x)$. That is

$$Y(x) = \mu(x) + Z(x). \tag{1}$$

Also, with the Maximum likelihood, we determine the covariance kernel adjustment parameters [6,7]. Thus, the covariance of $Z(x)$ is a known.

The first step for implementing the Kriging surrogate is to determine a design of experiments (DOE). The DOE is a distribution of points (samples) that fulfill the sample space, randomly generated by the Latin Hypercube. The main idea of the DOE is to divide each variable into an equal number of points to be sampled. Yet, we ensure that each compartment contains a single orthogonal projection of these points. However, this characteristic does not guarantee an adequate distribution of those points in the design space. In this sense, the Morris-Mitchell [6,7] criterion optimizes the Latin Hypercube. By following this criterion, the plan with the best design space is the one that maximizes the smaller distance between any pair of points inside the sample used [8].

The association of the DOE's points with the design variables used in the optimization problem gives them a physical sense. Each DOE's point is used in a finite element simulation. This simulation analyses the structural behavior following a given configuration of boundary conditions. Each simulation allows obtaining an output variable represented, for example, by displacements or stresses. With this output variable, one can evaluate the objective function of the problem. The output variable used in this study is the frequency response function obtained as the system's response in vertical acceleration (inertance). The objective function computes the Euclidean norm of a component of the matrix function of inertance as

$$f(x) = \sqrt{\int_{\Omega_i}^{\Omega_f} |A_{jk}(\Omega)|^2 \, d\Omega} \cong \sqrt{\Delta\Omega \sum_{j=1}^{ni} |A_{jk}(\Omega)|^2}, \tag{2}$$

being $\Delta\Omega = \Omega_f - \Omega_i$ and Ω_i and Ω_f the initial and final values of the frequency range in study. The term $A_{jk}(\Omega)$ is the function of inertance obtained for a vibrating harmonic system, sampled for n_i values of frequency, and follows

$$A_{jk}(\Omega) = \frac{-\Omega^2 X_j(\Omega)}{F_k(\Omega)}, \tag{3}$$

where $F_k(\Omega)$ is the component of the excitation force vector performed in the *k*-th degree of freedom. Also, $X_j(\Omega)$ is the component of the response vector in the *j*-th degree of freedom.

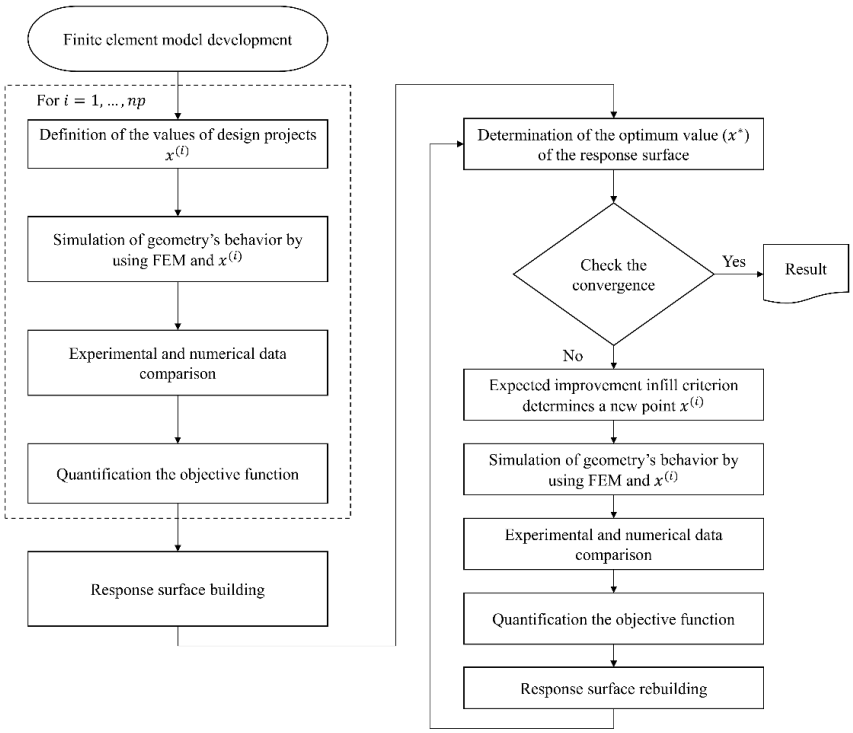

Figure 1. Flowchart of the optimization process

After evaluating each DOE point (samples), it is possible to build a response surface (surrogate) that represents the behavior of the objective function as the design variables change. After finishing the initial building of the surrogate, the optimization process continues by adding new points through an infill criterion. In this case, we use the expected improvement ($E[I(x)]$). In this criterion, we add new points $x^{(i)}$ to the known ones. So, the answer obtained by the surrogate fits as close as possible to the physical system. The choice of the new points follows an improvement measure ($I(x)$) given as [8]

$$I(x) = \begin{cases} y_{min} - y(x) & if \quad y(x) < y_{min}, \\ 0 & if \quad y(x) \geq y_{min} \end{cases} \tag{4}$$

being $y(x)$ the value of $f(x)$ found for the point added and y_{min} is the lowest value of $f(x)$ obtained on the surrogate. However, the value of this improvement in not previously known, because $y(x)$ is unknown. Thus, the equation that describes the expected improvement ($E[I(x)]$) is given by

$$E[I(x)] = \begin{cases} \left(y_{min} - \hat{y}(x)\right)\Phi\left(\dfrac{y_{min} - \hat{y}(x)}{\hat{s}(x)}\right) + \hat{s}(x)\phi\left(\dfrac{y_{min} - \hat{y}(x)}{\hat{s}(x)}\right) & if \quad \hat{s}(x) > 0, \\ 0 & if \quad \hat{s}(x) = 0. \end{cases} \tag{5}$$

In this equation, $\hat{y}$ and $\hat{s}^2$ are Kriging parameters and represent the prediction in a non-sampled point and an error estimator of the surrogate [8]. Also, Φ represents the cumulative distribution function and ϕ is the Gaussian probability density function.

A characteristic of the infill criterion is that E is null for known points. Another characteristic is the search in regions with little or no exploitation. The criterion value increases with the standard deviation between analytical and approximate functions. Besides, there is an increase in the criterion's magnitude in regions where the average of the functions is low. Finally, there is no need to know the minimum value of the objective function [6,7].

In this study, the Latin Hypercube fulfills the design space with 50 points. Thus, we built the initial response surface by determining $f(x)$ for all these points that compose the DOE. After building the initial surface response, the optimization problem assessed whether the stopping or convergence criteria were satisfied. The stopping

criterion refers to the maximum number of iterations that is 100. The convergence criterion refers to an improvement of $f(x)$ in a 10-iterations interval less than 1% of the objective function determined for the plate without vibration control. The optimization process finishes when any criterion is reached. Otherwise, the expected improvement infill criterion adds a new point, and the optimization continues. So, we evaluated $f(x)$ with this new value of $f(x)$ and built a new response surface. This process continues until the optimization reaches at least one criterion.

2.2 Optimization problems

The optimization problem used in this study considers two design variables to describe the design space. These variables are the thicknesses of VEM and constraining layer. The optimization problem follows

$$\begin{aligned} &minimize\ f(x) = \sqrt{\Delta\Omega \sum_{j=1}^{ni} \left|A_{jk}(\Omega)\right|^2}, \\ &subject\ to\ \ x_{low}^{(i)} \leq x\ \leq x_{upp}^{(i)} \quad (i = 1,2), \end{aligned} \tag{6}$$

$x_{low}^{(i)}$ and $x_{upp}^{(i)}$ are the values of upper and lower limits for *i*-th design variable. We present such limits in the results section for each CR considered in this study.

2.3 Geometric and finite element models

We used the geometries and their respective finite element mesh presented in Fig. 2. Three parts compose each model: (i) base structure, (ii) VEM, and (iii) constraining layers. The base structure has length, width, and thickness equal to 500 mm, 200 mm, and 25 mm. Both base structure and constraining layer are made of steel ASTM-A36 with elastic modulus, Poisson's ratio, and density equal to 210 GPa, 0.3, and 7,860 kg/m³.

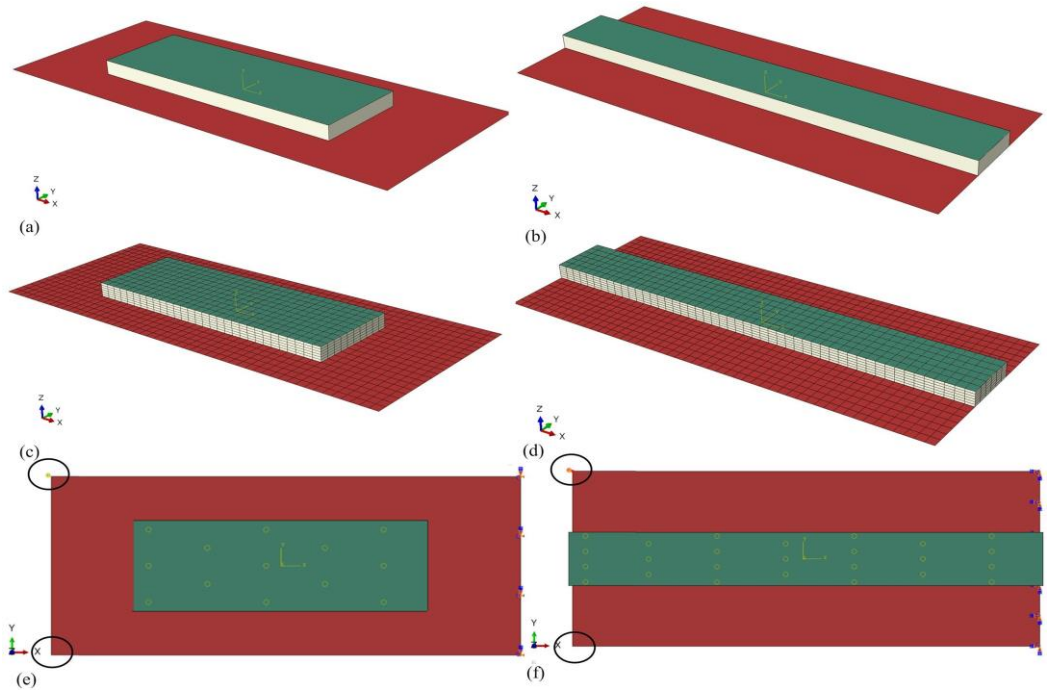

Figure 2. Centralized (a,c,e) and extended (b,d,d) contrained-layer models. (a-b) Geometries, (b,d) their finite element meshes, and (e,f) boundary conditions.

This work considered two types of CL. Both covered 30% of the base structure's total area. For both cases, the boundary condition is a fixed-right-edge base structure. In the first case, we used a CL centralized on the base structure (Fig. 2a). The CL has a length and width of 300 mm and 100 mm. In the second case (Fig. 2b), we modeled the CL longitudinally disposed on the base structure. However, the CL extended and centralized itself

along the length and width of the base structure. This configuration has dimensions (length and width) of 500 mm and 60 mm.

Shell elements S4R (shell, 4-nodes with reduced integration) discretize the base structure and constraining layer. Solid elements C3D8RH (continuum, 3D, 8-nodes with reduced integration, and hybrid[1]) discretize the VEM layer. Solid elements accurately represent the shear deformation of the VEM [9]. The mesh presents 3,100 elements and 3,927 nodes (Fig. 2c and 2d). We used a fixed number of elements to discretize the thickness of the VEM layer. In this sense, only the element thickness changes as the thickness of the layer changes during the optimization process. Finally, tie constraints kept the parts united during the simulations.

For obtaining the inertance, we used a unit vertical force at the left-superior node (excitation node), and the response (inertance) was measured at the left-inferior node (response node) of the base structure (Fig. 2e and 2f). We used the Direct-solution steady-state analysis procedure to determine the inertance. This procedure solves the complete set of the model degrees of freedom at each excitation frequency. As the Abaqus software documentation, this is the procedure used when viscoelastic material is present in the model. The simulations to obtain the inertance considered the range of frequency from 0 to 580 Hz.

2.4 Viscoelasticity defined in frequency domain

Abaqus represents the viscoelastic behavior by using the generalized Maxwell model. The complex dynamic modulus $E(\Omega_{\mathrm{r}})$ of a given VEM in the frequency domain is defined as [11]

$$E(\Omega_r) = \mathrm{E}_{\mathrm{Re}}(\Omega_r) + iE_{Im}(\Omega_r). \tag{7}$$

Here, Ω_r is the reduced frequency, which follows [12]

$$\Omega_r = \alpha_T \Omega. \tag{8}$$

In Eq. (8), α_T is a constant defined as a shift factor. This constant describes the temperature dependence of the VEM. In this study, we did not consider any temperature dependence. The storage modulus $(E_{Re}(\Omega_r))$ follows

$$E_{Re}(\Omega_r) = E_\infty + \sum_{i=1}^{NT} \frac{(\Omega_r \tau_i)^2 E_i}{(\Omega_r \tau_i)^2 + 1}, \tag{9}$$

And the loss modulus $(E_{Im}(\Omega_r))$ follows [11,12]

$$E_{Im}(\Omega_r) = \sum_{i=1}^{NT} \frac{\Omega_r \tau_i E_i}{(\Omega_r \tau_i)^2 + 1}. \tag{10}$$

In Eq. (8) and (9), NT represents the total number of terms of the Prony series, τ_i is the relaxation time associated to the i-th component of the generalized Maxweel model, $E_i$is the elastic constant, and E_∞ is the equilibrium modulus (this represents the pure elastic response only) [11,12].

Both $E_{Re}(\Omega_{\mathrm{r}})$ and $E_{Im}(\Omega_r)$ indicates how the material's behavior approaches the elastic or viscous behavior. In this case, the ratio between loss and storage modulus defines the loss factor η as [11,12]

$$\eta(\Omega_r) = \frac{E_{Im}(\Omega_r)}{E_{Re}(\Omega_r)}. \tag{11}$$

The loss factor η quantifies the ratio between dissipated and storage energies by the material in a cycle. Thus, we can rewrite the Eq. (7) as [11,12]

[1] Hybrid elements are used when the material behavior is incompressible or very close to incompressible. Pressure stress in the element is indeterminate. Thus, an incompressible material response cannot be modeled with regular elements (except in the case of plane stress). Incompressible materials do not change its volume under pressure stress. Therefore, the pressure stress cannot be computed from the displacements of the nodes. Thus, a pure displacement formulation is inadequate. Hybrid elements include an additional degree of freedom that determines the pressure stress for incompressible materials. The nodal displacements are used only to calculate the deviatoric (shear) strains and stresses [10].

$$E(\Omega_r) = \mathrm{E_{Re}}(\Omega_r)[1 + i\,\eta(\Omega_r)\,]. \tag{12}$$

Both $E_{Re}(\Omega_r)$ and η describe the dynamic properties of the material. Abaqus standard, through the direct-solution steady-state analysis procedure, determines the VEM's frequency-dependent behavior. The characterization of $E_{Re}(\Omega_r)$ and $E_{Im}(\Omega_r)$ in Abaqus depends on the terms of the Fourier transform (complex) $E^*(\Omega_\mathrm{r})$ of the nondimensional relaxation function [10]

$$E(t) = \frac{E_r(t)}{E_\infty} - 1, \tag{13}$$

by following

$$\mathrm{E_{Re}}(\Omega_r) = E_\infty[1 - \Omega_r\,\Im(E^*)], \tag{14}$$

and

$$E_{Im}(\Omega_r) = E_\infty[\Omega_R\,\Re(E^*)]. \tag{15}$$

In Eq. (13), $E_r(t)$ is the time-dependent elastic modulus. In Eq. (14) and (15), $\Im(E^*)$ and $\Re(E^*)$ are the real and imaginary parts of $E^*(\Omega_\mathrm{r})$. We defined the frequency dependency viscoelastic properties by using the tabular form through the definition of $\Omega_r\,\Im(E^*)$ and $\Omega_R\,\Re(E^*)$. The VEM used is the elastomer BT806-55 [13]. The reference temperature and VEM's density were equal to 30ºC and 1,289 kg/m³. Finally, Abaqus needs the characterization of the elastic behavior of the material [10]. For this, long-term elastic modulus (E_∞) and Poisson's ratio (ν) received values equals to 23.15 MPa and 0.495, for the same reference temperature.

3 Results e discussions

In the optimization process, we considered three upper limits for the constraining layer thickness for each geometry used. Table 1 presents these values. The main idea is to evaluate the influence of the constraining layer thickness on the optimization process and vibration control. The lower limit for describing the smaller thickness allowed was equal to 5.0 mm for the VEM and constraining layers.

Figure 3 presents the response function of inertance for the six optimization problems considered. We obtained the system without vibration control (dashed curves showed in Fig. 3) for a model without the CL. The range of frequency (0 to 580 Hz) comprehends the three first modes of vibration of the base structure with natural frequencies equal to 84.64 Hz, 399.15 Hz, and 514.26 Hz.

The CLs performed effective control, for all optimization cases, mainly for the second and third vibration modes. The reduction of the constraining layer thickness decreased the intensity of the vibration control performed. But, even low, there is a reduction in the amplitude of inertance. The CLs presented little or no influence on the first mode of vibration. The cases P1C1 and P2C1 presented the best results. Here, there was a decrease in the natural frequency associated with the first mode and a reduction of the amplitude of inertance. For the other cases, the CLs did not generate meaningful changes.

Table 1. Upper limits allowed for the VEM and constraining layer thicknesses during the optimization

Model	Optimization case	MVE thickness (mm)	Constraining layer (mm)
Centralized CL	P1C1	50.0	25.0
	P1C2	50.0	12.7
	P1C3	50.0	5.0
Extended CL	P2C1	50.0	25.0
	P2C2	50.0	12.7
	P2C3	50.0	5.0

Table 2 presents the optimum values for the VEM and constraining layers thicknesses. The optimization process indicated an increase in the VEM thickness for the cases where the upper limit of the constraining layer decreased. Another factor associated with the reduction of the constraining layer thickness is the value of the objective function (Tab. 2). One can note an increasing tendency as presented in the curves of inertance (Fig. 3c, 3d, 3e, and 3f). In the cases studied, a thicker constraining layer restrained the VEM's vertical movement.

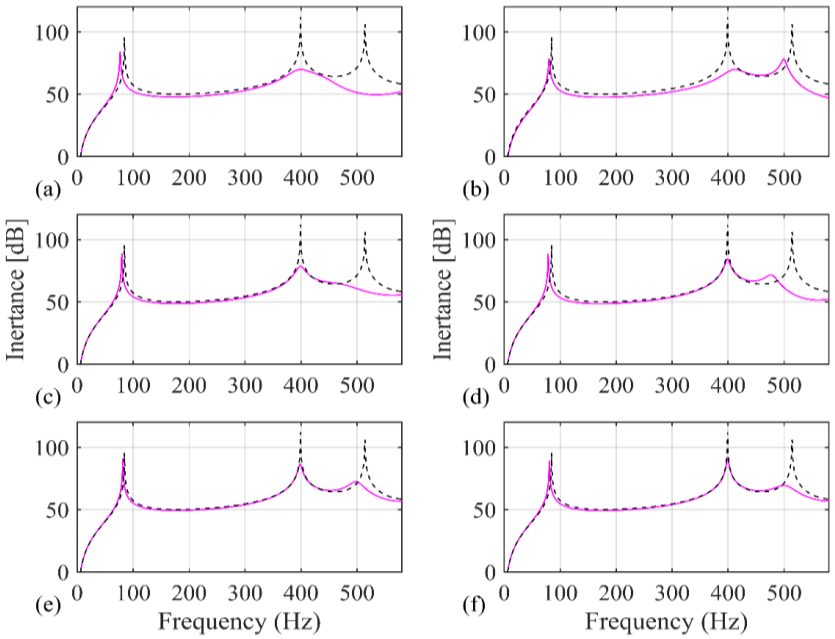

Figure 3. Inertance (dB) for (a,c,e) centralized and (b,d,f) extended CL. Continuum and dashed lines represent the plate with and without CL. Optimization cases: (a) C1P1, (b) C2P1, (c) C1P2, (d) C2P2, (e) C1P3, and (f) C2P3.

Table 2. Optimum VEM and CR thickness obtained for each optimization case and the objective function value

Model	Optimization case	Optimized MVE thickness (mm)	Optimized CR thickness (mm)	Objective function value (dB)
Centralized CL	P1C1	10.64	25.0	92.42
	P1C2	16.06	12.65	96.86
	P1C3	25.76	4.54	100.42
Extended CL	P2C1	0.5	25.0	94.80
	P2C2	10.05	12.63	99.18
	P2C3	18.96	5.0	102.40

An optimization problem allows to obtain a CL's optimum configuration (shape, quantity, and thicknesses of the VEM and constraining layers) for vibration control. A random configuration can cause the opposite effect. That is, it can increase the amplitude of inertance in the natural frequencies. One can visualize this when the constraining layer thickness tends to a small value.

One can note both CLs geometries presented an effective control for the second and third modes of vibration, even in the case of the thinnest CL. For the first mode, the extended CL geometry presented the best results, even with a low improvement about the first geometry. The extended CL has material closer to the fixed region. A high level of strain in the fixed region characterizes the first mode. In this sense, a large quantity of VEM in this region could be necessary for performing the control of the first mode. One can visualize this aspect by comparing the inertance obtained for the cases of the thicker CLs (Fig. 3a and 3b). With this in mind, the CL's localization is a

relevant design variable to be included in the optimization problem. We expect a meaningful improvement in the vibration control for the frequencies close to the first natural frequency of the system. Another situation is to use more than one CL over the base structure. Thus, the distribution of different quantities of VEM could perform the vibration control.

Despite the little control by frequencies close to the first mode, it is still possible to control the other modes. One can visualize the high or the low levels of control as the VEM and constraining layer change. We observe this behavior with the results obtained.

Although there is a vibration control, the geometries used did not represent the best possible configuration for controlling the vibration problem. That is, for the entire frequency range. In this sense, it is interesting to develop the shape or topology optimization of the CL. Just the addition of materials is not sufficient for this type of problem. The CL needs an optimum shape and a specific localization for performing the vibration control [1,14,15].

4 Conclusions

This study presented an optimization methodology using the Kriging surrogate to determine the optimum VEM and constraining layer thicknesses for vibration passive control. We evaluated two geometries with fixed dimensions (length and width). In both cases, we considered a fixed-right-edge structure. The methodology was applied for bandwidth control by comprehending the first three vibration modes.

One can note the obtained results did not present an effective control over the frequency range (0 to 580Hz). An important aspect is that the optimum thickness generates low or no vibration control for the first vibration mode. Nevertheless, we obtained a reduction of 30 dB for the second and third modes. Despite the simple CL configurations and that there is not an effective control for the first mode, we can classify the obtained results as satisfactory. Furthermore, the CR configurations avoid the checkerboard formation. This phenomenon usually occurs in structural topology optimization.

Acknowledgements. The authors thank the Post-Graduated Program in Mechanical Engineering (PG-Mec) from Federal University of Paraná (UFPR), Brazil. Furthermore, Sandmara Lanhi thanks the Programa de Recursos Humanos da Agência Nacional de Petróleo, Gás Natural e Biocombustíveis (PRH-ANP) for her financial support.

Authorship statement. The authors hereby confirm that they are the sole liable persons responsible for the authorship of this work, and that all material that has been herein included as part of the present paper is either the property (and authorship) of the authors or has the permission of the owners to be included here.

References

[1] R. Chen, H. Luo, H. Wang and W. Zhou, "Topology optimization of partial constrained layer damping treatment on plate for maximizing modal loss factors". *Composite and Advanced Materials*, vol. 30, pp. 1-19, 2021.
[2] J. F. A. Madeira, A. L. Araújo, C. M. Mota Soares and C. A. Mota Soares, "Multiobjective optimization for vibration reduction in composite plate structures using constrained layer damping". *Computers and Structures*, vol. 232, pp. 1-9, 2020.
[3] M. R. Permoon and T. Farsadi, "Free vibration of three-layer sandwich plate with viscoelastic core modelled with fractional theory". *Mechanics Research and Communications*, vol. 116, pp. 1-7, 2021.
[4] H. Wang, H. P. Lee and C. Du, "Analysis and optimization of damping properties of constrained layer damping structures with multilayers". *Shock and Vibration*, vol. 2021, pp. 1-11, 2021.
[5] D. Zhang, T. Qi and L. Zheng, "A hierarchical optimization strategy for position and thickness optimization of constrained layer damping/plate to minimiza soud radiation power". *Advances in Mechanical Engineering*, vol. 10, pp. 1-15, 2018.
[6] A.I.J. Forrester, A. Sóbester, A.J. Keane, A.J. *Engineering Design Via Surrogate Modelling: A Practical Guide.* John Wiley & Sons, 2008.
[7] O. Roustant, D. Ginsbourger, Y. Deville. "DiceKriging, DiceOptim: Two R packages for the analysis of computer experiments by Kriging-based metamodeling and optimization". *Journal of Statistical Software*, vol. 51, pp. 1–5, 2013.
[8] A.I.J. Forrester, A. Sóbester, A.J. Keane, A.J. "Multi-fidelity optimization via surrogate modelling". *Proceedings of the Royal Society A: Mathematical, Physical, and Engineering Sciences,* vol. 463, pp. 3251-3269, 2007.
[9] C. Xu, S. Lin and Y. Yang, "Optimal design of viscoelastic damping structures using layerwise finite element analysis and multi-objective genetic algorithm". *Computers and Structures*, vol. 157, pp. 1-8, 2015.
[10] Abaqus v. 6.14 Documentation.

[11] E.M.O. Lopes, C.A. Bavastri, J.M.S. Neto, and J.J. Espíndola, "Characterization dynamics in integrated elastomers generalized derivatives, in: *Proceedings of the III CONEM,* Belem, 2004.
[12] T. L. Sousa, F. Kanke, J. T. Pereira, and C. A. Bavastri, "Property identification of viscoelastic solid materials in nomograms using optimization techniques", *Journal of Theoretical and Applied Mechanics*, vol. 55, pp. 1285-1297, 2017.
[13] Olienick, E.G. F., E. M. O. Lopes, and C. A. Bavastri, "Integrated dynamic characterization of thermorheologically simple viscoelastic materials accounting for frequency, temperature, and preload effects", *Materials*, 12, pp. 1962, 2019.
[14] F. Kanke, Otimização Topológica de Camadas Restritoras Aplicada ao Controle de Vibrações em Placas Semi-Espessas, Dissertation, Federal University of Paraná, 2017.
[15] M. Kolk, G. Veen, J. Vreugd and M. Langelaar, "Multi-material topology optimization of viscoelastically damped structures using a parametric level set method". *Journal of Vibration and Control*, vol. 23, n.15, pp. 1-14, 2017.